Molecular Biology Reports (2020) 47:2061–2071
https://doi.org/10.1007/s11033-020-05306-9

ORIGINAL ARTICLE

Targeting signaling pathways of VEGFR1 and VEGFR2 as a potential target in the treatment of breast cancer

Maryam Farzaneh Behelgardi[1] · Saber Zahri[1] · Zahra Gholami Shahvir[2] · Farhad Mashayekhi[2] · Laleh Mirzanejad[2] · S. Mohsen Asghari[2,3]

Received: 25 September 2019 / Accepted: 5 February 2020 / Published online: 18 February 2020

Abstract

Tumor angiogenesis allows tumor cells to grow and migrate toward the bloodstream and initiate metastasis. The interactions of vascular endothelial growth factors (VEGF) A and B, as the important regulating factors for blood vessel growth, with VEGFR1 and VEGFR2 trigger angiogenesis process. Thus, preventing these interactions led to the effective blockade of VEGF/VEGFRs signaling pathways. In this study, the inhibitory effect of a 23-mer linear peptide (VGB4), which binds to both VEGFR1 and VEGFR2, on VEGF-stimulated Human Umbilical Vein Endothelial Cells (HUVECs) and highly metastatic human breast cancer cell MDA-MB-231 proliferation was examined using MTT assay. To assess the anti-migratory potential of VGB4, HUVECs and also MDA-MB-231 cells wound healing assay was carried out at 48 and 72 h. In addition, downstream signaling pathways of VEGF associated with cell migration and invasion were investigated by quantification of mRNA and protein expression using real-time quantitative PCR and western blot in 4T1 tumor tissues and MDA-MB-231 cells. The results revealed that VGB4 significantly impeded proliferation of HUVECs and MDA-MB-231 cells, in a dose- and time-dependent manner, and migration of HUVECs and MDA-MB-231 cells for a prolonged time. We also observed statistically significant reduction of the transcripts and protein levels of focal adhesion kinase (FAK), Paxillin, matrix metalloproteinase-2 (MMP-2), RAS-related C3 botulinum substrate 1 (Rac1), P21-activated kinase-2 (PAK-2) and Cofilin-1 in VGB4-treated 4T1 tumor tissues compared to controls. The protein levels of phospho-VEGFR1, phospho-VEGFR2, Vimentin, β-catenin and Snail were markedly decreased in both VGB4-treated MDA-MB-231 cells and VGB4-treated 4T1 tumor tissues compared to controls as evidenced by western blotting. These results, in addition to our previous studies, confirm that dual blockage of VEGFR1 and VEGFR2, due to the inactivation of diverse signaling mediators, effectively suppresses tumor growth and metastasis.

Keywords VEGF · VEGFR1 · VEGFR2 · Antagonist peptide · Breast cancer · Migration

Introduction

Tumor angiogenesis is necessary for tumor growth and metastasis. Among angiogenesis modulating growth factors, vascular endothelial growth factor (VEGF) (also known as VEGF-A) has a dominant role by inducing endothelial cell proliferation, migration, invasion and capillary tube formation [1].

Cell migration as a hallmark of angiogenesis and metastasis is initiated by plasma membrane protrusions consisting of large lamellipodia, finger-like filopodia or both on the leading edge. These protrusions are driven by actin filaments polymerization followed by focal adhesion assembly, tractional forces generation, and tail retraction and detachment [2]. Growth factor receptors and integrins regulate the

Electronic supplementary material The online version of this article (https://doi.org/10.1007/s11033-020-05306-9) contains supplementary material, which is available to authorized users.

✉ S. Mohsen Asghari
sm_asghari@guilan.ac.ir

[1] Department of Biology, Faculty of Science, University of Mohaghegh Ardabili, Ardabil, Iran

[2] Department of Biology, Faculty of Science, University of Guilan, Rasht, Iran

[3] Institute of Biochemistry and Biophysics (IBB), University of Tehran, Tehran, Iran

VEGF stimulated endothelial cell migration [3]. In particular, VEGF induces tyrosine phosphorylation of focal adhesion associated proteins in focal adhesions [4], where link extracellular matrix to actin cytoskeleton [5]. FAK and Paxillin are prominent components localized in focal adhesions essential for actin filament assembly and cell motility [6].

FAK, a multi-domain non-receptor tyrosine kinase, acts as the key signaling molecule involved in cell proliferation, migration and survival [7]. Although FAK mostly participates in integrin-mediated signaling, several studies have shown its activation in response to stimulations of growth factors [7–9]. FAK activation triggers multiple downstream signaling pathways through the recruitment and phosphorylation of adaptor proteins such as paxillin in focal adhesion [10]. Paxillin, a multi-domain adaptor protein, plays a key role in several signaling pathways [11]. The structural characteristics of paxillin allow to act as a docking site and an important scaffolding component for the other signaling molecules involved in cell migration and adhesion [11]. PAKs, multi-domain non-receptor serine/threonine kinases, are recruited to focal adhesion through binding to adaptor proteins such as paxillin and localized immediately in downstream of small GTPases (Rac1/cdc42), and regulate the cellular activities, e.g. actin cytoskeleton remodeling, motility and invasion [12, 13]. Numerous investigations have shown the overexpression of the mammalian PAK family, including PAK-1 to -6, in human breast tumors [14–16]. LIM-kinases (LIMKs) and actin-binding kinases activated by PAKs, phosphorylate and inactivate cofilin. Inhibition of cofilin activation stabilizes F-actin filaments [17]. In particular, active Cofilin serves as depolymerizing and severing of F-actin. Therefore, local activation of Cofilin reduces efficiency of cell protrusion [18]. PAKs also upregulatethe expression of MMPs [19] , a family of Zn^{2+}-dependent proteolytic enzymes which digest the extracellular matrix (ECM) components and break down basement membrane. The increase in the levels of circulating MMPs is associated with breast cancer invasion and metastasis [20, 21].

Snail is a zinc-finger containing transcription factor which is associated with breast tumor migration and invasion through the induction of Epithelial-Mesenchymal Transition (EMT) [22]. The key events in EMT cellular process are disorganization of E-cadherin-β-catenin complex and de novo expression of mesenchymal marker, Vimentin [22, 23].

We have previously reported a VEGF-antagonistic peptide (denoted as VGB4) that its binding to both VEGFR1 and VEGFR2 led to the abrogation of VEGF-mediated signaling pathways, appreciable inhibition of tumor angiogenesis, growth, and metastasis [24]. The aim of current study is to investigate the effect of VGB4 on metastatic pathways in human breast cancer cell MDA-MB-231 and 4T1 tumor tissue. Our findings demonstrate the significant decrease of VEGFR1 and VEGFR2 phosphorylation resulting in destabilization of focal adhesions and disruption of actin organization through downregulation of FAK-Paxillin-MMP-2 as well as Rac-PAK-Cofilin pathways, and downregulation of Vimentin, Snail and β-catenin (EMT markers) in VGB4-treated breast tumors. These results suggest that antimigratory and antiinvasive potential of VGB4 can be due to simultaneous blocking of VEGFR1 and VEGFR2.

Material and methods

Peptide and antibodies

The peptide was synthesized and purified by high-performance liquid chromatography (HPLC) at a purity of 90%, analyzed by matrix-assisted laser desorption/ionization time-of-flight mass spectrometry (MALDI-TOF), and approved by electrospray ionization mass spectrometry (ESI–MS) analysis (Shine Gene Biotechnologies, Inc., Shanghai, China). Anti-phospho-VEGFR1 (SAB4504006), anti total-FAK (SAB4502500), anti total-Cofilin (SAB2702206), anti phospho-PAK-2 (SAB4504634) and anti total-PAK-2 (SAB4502071) were from Sigma (St Louis, MO, USA); anti-GAPDH (sc-32233) was purchased from SANTA CRUZ BIOTECHNOLOGY, INC., Santa Cruz, California, USA; Goat Anti-Rabbit IgG H&L (HRP) (ab205718), Donkey Anti-Goat IgG H&L (HRP) (ab205723), anti-Rac1 (ab97732), anti-Vimentin (ab137321), anti-β-catenin (ab2365), anti-Snail (ab53519), anti phospho-Cofilin (ab12866) and anti-phospho-VEGFR2 (ab194806) were purchased from Abcam, Cambridge, UK. Anti-phospho-FAK (# 44-624G) was from Invitrogen (Carlsbad, CA). Anti-phospho-Paxillin (#2541) and anti total-Paxillin (#2542) were purchased from Cell Signaling Technology. Rac activation assay kit was from Cell Biolabs, (San Diego, CA).

Cell culture

HUVEC (NCBI code: C554) and MDA-MB-231 cell (NCBI code: C578) were purchased from the National Cell Bank, Pasteur Institute of Iran, cultured in Dulbecco's Modified Eagle's Medium (DMEM; Gibco, Life Technologies, USA), and supplemented with 10% fetal bovine serum (FBS; Sigma, St. Louis, Missouri, USA). The culture was incubated at 37 °C and 5% CO_2 until the confluency reached about 90%.

MTT assay

4×10^4 MDA-MB-231cells and 3×10^3 Human Umbilical Vein Endothelial Cells (HUVECs) were cultured in DMEM medium supplemented with 10% FBS into a 24-well plate. The medium was replaced with the media supplemented

with 2% FBS, 200 ng/ml VEGF-A (Sigma, St. Louis, Missouri, USA) and various concentrations (0.09, 0.18, 0.37, 0.55 and 0.74 µM) of VGB4 or (0.74 µM) of scr. After 24, 48 and 72 h incubation, 5 mg/ml of 3-(4,5-dimethylthiazol-2-yl)-2,5-diphenyltetrazoliumbromide (MTT) (Sigma, St. Louis, Missouri, USA) was added and the plates were incubated for 4 h at 37 °C. Then, dimethyl sulfoxide (DMSO) (100 µl) was added to the plate to solubilize the purple formazan crystals. The absorbance was read at 570 nm by an ELISA plate reader.

Wound healing migration assay

3×10^3 HUVEC and 3×10^4 MDA-MB-231 cells were seeded and grown in a 24-well culture plate. The confluent monolayer was wounded using a sterile 100 µl pipette tip to generate a cell-free area. After washing with PBS, the medium was replaced with the medium containing 2% FBS and concentrations (0.37 and 0.74 µM) of VGB4 or (0.74 µM) of scr and 200 ng/ml VEGF-A. The rate of wound closure was monitored microscopically after 48 h and 72 h, given that the percentage of migration = 0 at 0 h. Images were taken using the camera connected to an inverted microscope (Olympus BX-50, Japan). The wound area was measured by Wimasis image analysis software (https://www.wimasis.com/en/).

Animals

In our previous animal study [24], for assessment of the efficacy of VGB4 peptide in a 4T1 breast tumor model, we aseptically excised murine 4T1 mammary carcinoma tumors from BALB/c mice-bearing breast cancer and cut them into the small pieces, approximately 0.3 cm^3. After subcutaneous transplantation of tumor pieces to the 4–6 week-old female BALB/c mice, when the tumor volume reached ~ 200 mm^3 on the 14th day, the intraperitoneal injection of VGB4 peptide was started for 2 weeks. Treatment groups daily received different doses of VGB4 or scr peptide and control group received equal volume of PBS. After a 2-week treatment, the tumor tissue sections removed from the BALB/c mice treated with 5 mg/kg and 10 mg/kg doses of VGB4, and 10 mg/kg dose of scr were kept in − 70 °C and we, in the present study, used these frozen tumor tissue sections for Real-time quantitative polymerase chain reaction and western blot.

Real-time quantitative PCR

Total RNA was isolated from tumor tissue samples using the TRIZOL reagent (Invitrogen, Carlsbad, CA) based on the manufacturer's instruction. The purity and concentration of RNA were determined using 1% agarose gel electrophoresis and Nano Drop instrument (Thermo-Ones, Wilmington, DE). Complimentary DNA (cDNA) synthesis was performed using Revert Aid First strand cDNA synthesis kit (ThermoFisher, Waltham, MA) based on the protocol manual. The primer sequences of FAK, Paxillin, PAK-2, Cofilin-1, MMP-2, Rac1 and Glyceraldehyde-3-phosphate dehydrogenase (GAPDH) genes were designed by Oligo 7 primer analysis software (Table 1). In a thin walled PCR reaction tube, 6.5 µl of SYBR green master mix (Bioron, GmbH) was added to 1 µl cDNA sample, 0.5 µl forward primer, 0.5 µl reverse primer and 4.5 µl sterile deionized water. RT-qPCR was performed on Roche *LightCycler® 96 Instrument* and the reaction condition was set at 94 °C for 5 min as an initial denaturation which followed by 30 cycles of denaturation at 94 °C for 30 s, annealing at 58 °C for 30 s and extension at 72 °C for 30 s; and a final extension at 72 °C for 5 min. At the end of the program, the melting curve was checked and the relative gene expression level was quantified using ΔΔCT (delta-delta CT) method by which the calculated mRNA level was represented as fold change value ($2^{-\Delta\Delta CT}$) in data analysis. GAPDH was also used as a suitable endogenous reference gene. All the primers used in RT-qPCR were synthesized by Pars Mehr Zist (Iran).

Western blot

MDA-MB-231 cells or 4T1 tumor tissues from control and VGB4-treated groups were lysed with RIPA buffer supplemented with protease and phosphatase inhibitor cocktail (Sigma, St. Louis, Missouri, USA). The lysate was then centrifuged at 4 °C and the protein concentration was assessed by Lowry method. Equal volumes of total proteins were separated by 10% sodium dodecyl

Table 1 Primer sequences used in RT-qPCR analysis

Gene	Strand	Primer sequence
FAK	Forward	5′-CCATGCCCTCGAAAAGCTATG-3′
	Reverse	5′-TGACGCATTGTTAAGGCTTCT-3′
Paxillin	Forward	5′-GGCATCCCAGAAAATAACACTCC-3′
	Reverse	5′-GCCCTGCATCTTGAAATCTGA-3′
PAK-2	Forward	5′-GTAACCGCTAACATCGTCACC-3′
	Reverse	5′-ACTGTCTCTTTACACCCCTC-3′
Cofilin-1	Forward	5′-TTTAACGACACCCCTACTCCG-3′
	Reverse	5′-TCCTGCTTCCATGAGTGGTC-3′
MMP-2	Forward	5′-AAGGATGGACTCCTGGCACATGCC TTT-3′
	Reverse	5′-ACCTGTGGGCTTGTCACGTGGTGT-3′
Rac1	Forward	5′-ACGGAGCTGTTGGTAAAACCT-3′
	Reverse	5′-AGACGGTGGGGATGTACTCTC-3′
GAPDH	Forward	5′-CCCATCACCATCTTCCAGGAGC-3′
	Reverse	5′-CCAGTGAGCTTCCCGTTCAGC-3′

sulfate–polyacrylamide gel electrophoresis and transferred to polyvinyl difluoride (PVDF) membranes (Sigma, St. Louis, Missouri, USA). After blocking with 5% non-fat milk, the membranes were incubated with the primary antibodies including anti-phospho-VEGFR1, anti-phospho-VEGFR2, anti-total-VEGFR1, anti-total-VEGFR2, anti-phospho-FAK, anti-total-FAK, anti-phospho-Paxillin, anti-total-Paxillin, anti-phospho-Cofilin, anti-total-Cofilin, anti-phospho-PAK2, anti-total-PAK2, anti-Vimentin, anti-β-catenin, anti-Snail and anti-GAPDH at 4 °C overnight, followed by the incubation with secondary HRP-conjugated anti-rabbit or anti-goat antibodies at room temperature for 1 h. The bands were visualized using ECL reagent (Amersham, GE Healthcare Bio-Sciences Corp, Piscataway, NJ, USA). GAPDH was used as the internal control. The quantification of protein bands with reference to GAPDH control bands was performed using Image J software (NIH Image, National Institutes of Health; online at: https://rsbweb.nih.gov/ij/).

Rac activation assay

Rac activation was assayed by using Cell Biolabs' Rac1 Activation Assay Kit. 4T1 tumor tissue lysates were prepared and then incubated with PAK–PBD Agarose beads for 1 h at 4 °C to pull down the active form of Rac (GTP-bound Rac1). The beads were washed three times with assay buffer, resuspended in SDS sample buffer, boiled and separated by 12% SDS–PAGE gel, and analysed for Rac1 by western blotting.

Gelatin gel zymography

To determine the enzymatic activity of MMP-2, gelatin gel zymography was carried out as described [25] with some changes. 4T1 tumor tissues were homogenized with lysis buffer (50 mM Tris/HCl pH 7.5, 75 mM NaCl, 1% Triton X-100 and 1 mM PMSF). Supernatant was incubated with 50% $(NH4)_2SO_4$ for 10 min. Pellets were resuspended in 220 µl 50 mM Tris/HCl buffer (pH 7.5) and then incubated with 100 µL Gelatine-Sepharose 4B beads (Amersham, GE healthcare, Pittsburgh, USA) at 4 °C for 2 h with gentle agitation. The collected beads were incubated with 200 µl of elution buffer (50 mM Tris/HCl, 15 mM $CaCl_2$, 1 M NaCl and 8% DMSO) for 1 h at 4 °C with shaking. The samples were separated on 10% SDS-PAGE gel. The gel was incubated in the fresh developing buffer (50 mM Tris/HCl, 10 mM $CaCl_2$, 0.02% NaN_3) for 42 h at 37 °C. Then the gel was stained with Coomassie blue R-250 for 30 min, and destained in destaining solution (25% methanol and 5% acetic acid) to detect the clear bands.

Statistical analysis

Statistical analyses were performed using GraphPad Prism7 software. Data normality was assessed with Kolmogorov–Smirnov test. The significant difference between groups was evaluated with Unpaired Student's t-test. Differences were considered statistically significant when $P < 0.05$.

Results

Peptide design

A 23-mer linear peptide (referred to as VGB4) was designed based on VEGF-B and VEGF-A regions involved in ligation to VEGFR1 and VEGFR2 [24]. The sequence of the designed peptide was $_2$HN-KQLVIKPHGQILMIRYPSSQLEM-COOH.

Dose- and time-dependent inhibition of VEGF-induced cell proliferation and migration

To determine the inhibitory effect of VGB4, we first assessed proliferation of HUVECs and MDA-MB-231 cells in the presence of 200 ng/ml VEGF-A using MTT assay. As shown in Fig. 1a, proliferation of VEGF-stimulated cells (positive control) was significantly increased at different time points (24, 48 and 72 h) compared to unstimulated cells (negative control) ($P < 0.001$). As indicated in Fig. 1a, VGB4 created a dose- and time-dependent inhibition of VEGF-stimulated proliferation so that the maximal inhibition was observed at 0.74 µM. The scrambled peptide (scr, 0.74 µM), however, could not suppress VEGF-induced proliferation of cells. The half-maximal inhibitory concentrations (IC_{50}) of VGB4 following incubation for 24, 48 and 72 h on HUVECs and MDA-MB-231 cells were at 0.74, 0.55 and 0.55 µM, respectively ($P < 0.001$). Based on a report by Lee et al. [26], Sorafenib, a known tyrosine kinase inhibitor (TKI), inhibited MDA-MB-231 cells proliferation with IC_{50} value of 10.752 µM. By comparison, VGB4 suppressed MDA-MB-231 cells proliferation with IC_{50} values of ~ 0.5 µM and 0.74 µM, indicating that VGB4 is about ten times more potent than Sorafenib. Next, wound healing assay was conducted to further assess the effect of VGB4 on endothelial and MDA-MB-231 cells migration at later time points (48

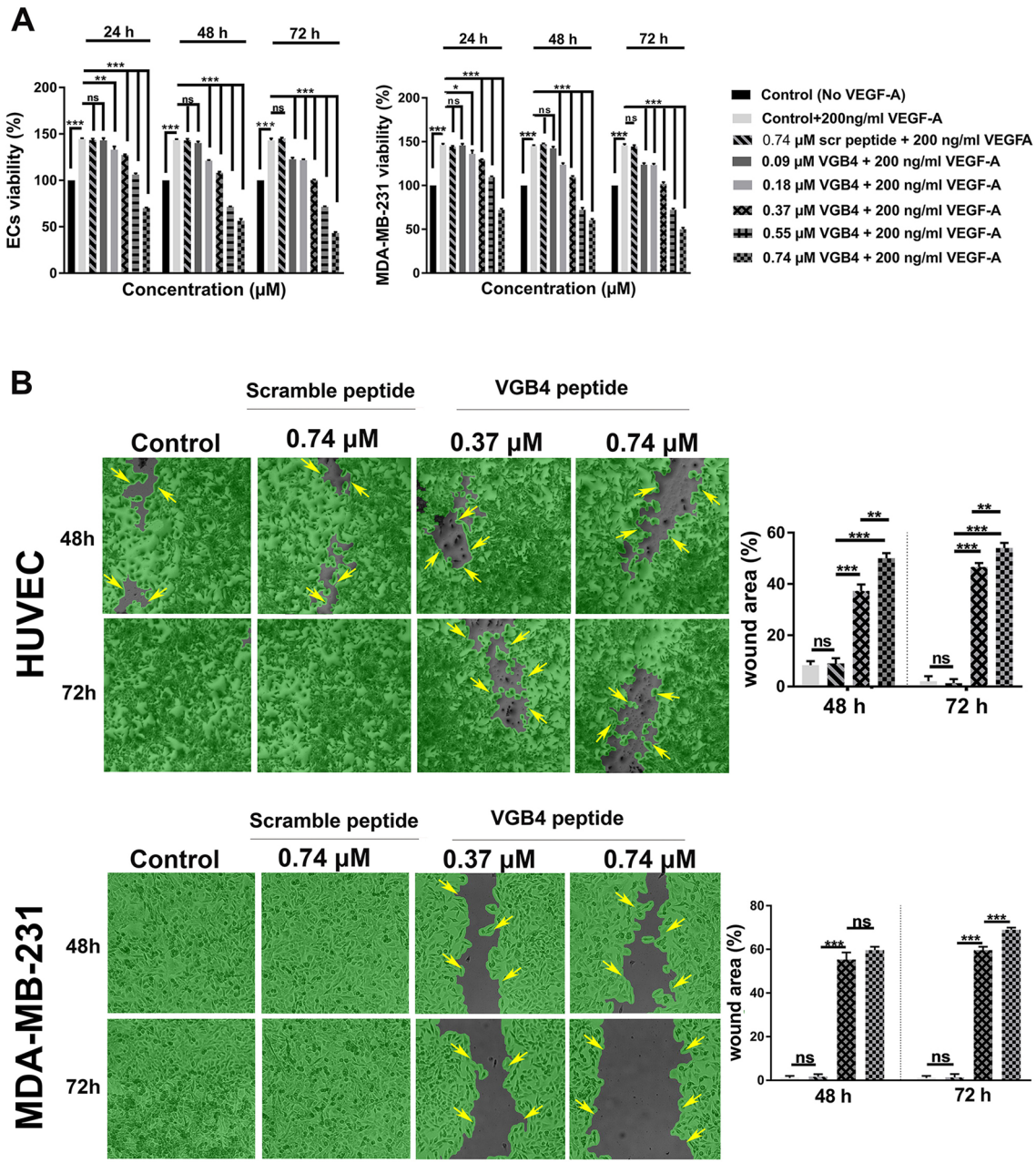

Fig. 1 The investigation of dose- and time- dependent anti-proliferative and anti-migratory properties of VGB4. **a** HUVECs and MDA-MB-231 cells were treated with various concentrations (0.09, 0.18, 0.37, 0.55 and 0.74 μM) of VGB4 for 24, 48 and 72 h in the presence of VEGF-A (200 ng/ml). **b** HUVECs and MDA-MB-231 cells were mechanically wounded and treated with 0.37 and 0.74 μM of VGB4, and 200 ng/ml VEGF-A for 48 h and 72 h. Image analysis was performed using Wimasis image analysis software. The grey areas in the images reveal the wound areas. Data were represented as mean ± SD, n = 3, $*P < 0.05$, $**P < 0.01$, $***P < 0.001$ compared to the control

and 72 h). The rate of wound closure was measured after 48 h and 72 h, revealing that VGB4 (0.37 and 0.74 μM) significantly decreased the wound closure rates compared with control and scr-treated cells ($P < 0.001$) (Fig. 1b). The percentage of wound area was measured by Wimasis Image Analysis (https://www.wimasis.com/en/).

RT q-PCR analysis of FAK, Paxillin, MMP-2, Rac1, PAK-2 and Cofilin-1 mRNA expression levels in VGB4-treated 4T1 tumor tissues

The melting and amplification curves analyses of the mRNA expression from RT q-PCR were carried out (Supplementary Fig. S1). The obtained average melting temperature (T_m) from melting curve analysis of FAK, Paxillin, MMP-2, Rac1,

PAK-2, Cofilin-1 and GAPDH genes are respectively as follows: 85.3 ± 0.2, 85.5, 85.1, 85, 88, 85 ± 0.3, and 89.8 (in untreated tumors), 85, 85.4, 85.1 ± 0.4, 87.6, 84.2 ± 0.3, 84.8 and 89.5 (in 10 mg/kg scr-treated tumors), 85, 85 ± 0.2, 84.8, 84.4, 88, 85 and 89.6 (in 5 mg/kg VGB4-treated tumors) and 85.2, 85.1 ± 0.3, 84.5, 85 ± 0.2, 87.8 ± 0.2, 84.5 and 90 (in 10 mg/kg VGB4-treated tumors). T_m peaks of the RT q-PCR products were also calculated by plotting the negative derivative of fluorescence over temperature (Supplementary Fig. S1). A single melting peak at a temperature along with the results of amplification curves analyses confirm specific amplification of the target genes (Supplementary Fig. S1). The results of primer efficiency calculation, with a mean E = 0.99 ± 0.05, were obtained for all genes. Furthermore, relative changes in mRNA expression levels of FAK, Paxillin, MMP-2, Rac1, PAK-2 and Cofilin-1 genes were quantified using RT q-PCR in VGB4-treated 4T1 tumor tissues

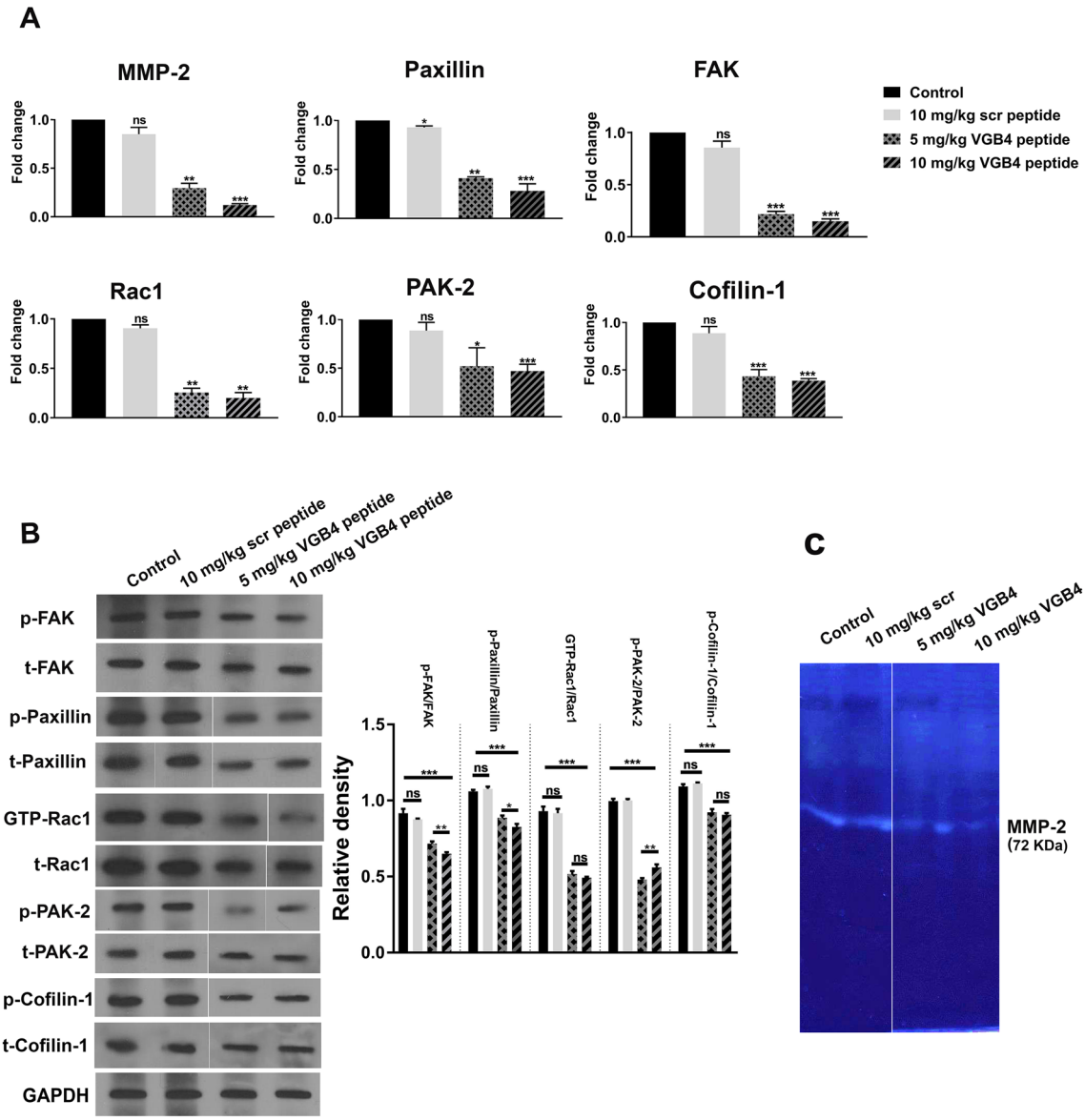

Fig. 2 RT q-PCR and western blot analysis of tissue mRNA and protein level of FAK, Paxillin, MMP-2, Rac1, PAK-2 and Cofilin-1 in 4T1 tumors. **a** The mRNA expression levels were determined in tumor tissue sections of untreated and VGB4 (5 mg/kg/day and 10 mg/kg/day)- or scr (10 mg/kg/day)- treated BALB/c mice. The relative mRNA expression levels were calculated using ΔΔCT method and normalized against GAPDH mRNA. **b** The protein levels of phospho-FAK, total-FAK, phospho-Paxillin, total-Paxillin, phospho-Cofilin, total-Cofilin, phospho-PAK-2, total-PAK-2 as well as GTP-Rac1 and total-Rac1 were assessed by western blot analysis. **c** Representation of gelatin zymography demonstrating down regulation of MMP-2 activity in VGB4-treated groups compared to controls. Data are expressed as the mean ± S.D. of three experiments. *P < 0.05, **P < 0.01, ***P < 0.001 versus control groups

compared to untreated tumor tissues and scr-treated tumors (Fig. 2a).

Tissue mRNA level of FAK

The qRT-PCR analysis revealed a significant difference in transcript level of FAK between VGB4-treated, untreated and scr-treated tumors ($P < 0.001$). As shown in Fig. 2a, VGB4 markedly reduced the expression level of focal adhesion kinase by 78.3% and 85.1% at doses 5 mg/kg and 10 mg/kg compared to controls, respectively.

Tissue mRNA level of Paxillin

The qRT-PCR analysis revealed a significant reduction in transcript level of Paxillin in VGB4-treated tumors compared to untreated and scr-treated tumors ($P = 0.005$ for 5 mg/kg/day, and $P < 0.001$ for 10 mg/kg/day). As shown in Fig. 2a, the mRNA level of Paxillin was decreased by 59% and 72% at doses 5 mg/kg and 10 mg/kg of VGB4 compared to controls, respectively. Paxillin mRNA levels were not statistically significantly different at doses 5 and 10 mg/kg/day of VGB4 ($P = 0.131$).

Tissue mRNA level of MMP-2

The qRT-PCR analysis revealed a dose-dependent reduction in transcript level of MMP-2 in VGB4-treated tumors compared to untreated and scr-treated tumors ($P = 0.002$ for 5 mg/kg/day and $P < 0.001$ for 10 mg/kg/day). As shown in Fig. 2a, the mRNA level of MMP-2 was decreased by 70.5% and 88.0% at doses 5 and 10 mg/kg/day of VGB4 compared to controls, respectively. The difference in the mRNA level of MMP-2 was found to be statistically significant between doses 5 and 10 mg/kg of VGB4 ($P = 0.041$).

Tissue mRNA level of Rac1

The RT q-PCR analysis revealed a significant reduction in transcript level of Rac1 in VGB4-treated tumors compared to untreated and scr-treated tumors ($P = 0.002$). As shown in Fig. 2a, the mRNA level of Rac1 was decreased by 75 and 80% at doses 5 mg/kg/day and 10 mg/kg/day of VGB4 compared to controls, respectively.

Tissue mRNA level of PAK-2

The qRT-PCR analysis revealed a reduction in transcript level of PAK-2 in VGB4-treated tumors compared to untreated and scr-treated tumors ($P = 0.012$ for 5 mg/kg/day, and $P < 0.001$ for 10 mg/kg/day). As shown in Fig. 2a, the mRNA level of PAK-2 was decreased by 48% and 53% at doses 5 and 10 mg/kg/day of VGB4 compared to controls, respectively. PAK-2mRNA levels were not statistically significantly different at doses 5 and 10 mg/kg/day of VGB4 ($P = 0.692$).

Tissue mRNA level of Cofilin-1

The qRT-PCR analysis revealed a significant reduction in transcript level of cofilin-1 in VGB4-treated tumors compared to untreated and scr-treated tumors ($P = 0.001$ for 5 mg/kg/day, and $P < 0.001$ for 10 mg/kg/day). As shown in Fig. 2a, the mRNA level of cofilin-1 was decreased by 56.7% and 61.4% at doses 5 and 10 mg/kg/day of VGB4 compared to controls, respectively.

The effect of VGB4 on FAK, Paxillin, Cofilin-1, PAK-2, Rac1, and MMP2 protein levels in 4T1 tumor tissues

Western blot analysis revealed a marked reduction in the expression levels of p-FAK, p-Paxillin, p-Cofilin-1, p-PAK-2, and GTP-Rac1 and total form of the proteins in VGB4-treated tumors relative to untreated and scr-treated tumors (Fig. 2b). The significant reduction in the ratio of phosphoproteins to total proteins in VGB4-treated tumors compared to control groups ($P < 0.001$), reveals that VGB4 could inhibit the phosphorylation of these proteins. Furthermore, MMP-2 gelatin zymography revealed a marked reduced MMP-2 activity in VGB4-treated 4T1 tumors compared to untreated control groups (Fig. 2c).

Analysis of VEGFR1, VEGFR2, β-catenin, Vimentin and Snail protein expression levels in VGB4-treated MDA-MB-231 cells and VGB4-treated 4T1 tumor tissues

The VEGF/VEGFR-1/-2 axes promote invasion and metastasis by promotion of EMT process in breast cancer cells [27]. The correlation between expression of VEGFR-2 and EMT biomarkers has become apparent [28]. Given that VEGFR-2 serves as a mediator of EMT in breast tumors, blocking of VEGFR-2/PI3K/Akt/Snail and β-catenin signaling is important in breast cancer treatment [29]. Likewise, several studies have found that the high level of VEGF/VEGFR-1/-2/NRP-1 axis in metastatic MDA-MB-231 and 4T1 cells regulates survival and invasion through maintaining the mesenchymal phenotype (up-regulated the levels of Vimentin and snail expression) [30, 31]. Therefore, interfering with VEGF/VEGFRs interaction inhibits VEGFR1 and VEGFR2 phosphorylation followed by the inactivation of VEGFRs signaling-mediated EMT. VGB4 is able to bind to both VEGFRs and inactivates downstream pathways associated with VEGF [24]. In this respect, the effect of VGB4 on major signaling pathways involved in VEGF-induced

EMT was further assessed in MDA-MB-231 cells and 4T1 tumor tissues and the level of phosphorylated-VEGFR1 (Y1313), phosphorylated-VEGFR2 (Y1175), Vimentin, β-catenin and Snail were determined using western blot analysis. As shown in Fig. 3a, VGB4 potently decreased p-VEGFR1, t-VEGFR1, p-VEGFR2 and t-VEGFR2 levels in 4T1 tumor tissues and MDA-MB-231 cells compared to control groups ($P < 0.001$). Furthermore, VGB4 significantly blocked Vimentin, β-catenin and Snail in 4T1 tumor tissues and MDA-MB-231 cells compared to controls ($P < 0.001$) (Figs. 3b, 4). These results further confirm the antagonizing property of VGB4 on VEGF-mediated cell invasion and metastasis.

Discussion

Simultaneous blockage of VEGFR1 and VEGFR2 inactivates broader signaling pathways of VEGF, thereby more effectively suppression of tumor growth and metastasis than blockade of VEGFR1 or VEGFR2 alone [32–35]. In particular, VEGFR2 is a pivotal regulator of angiogenesis.

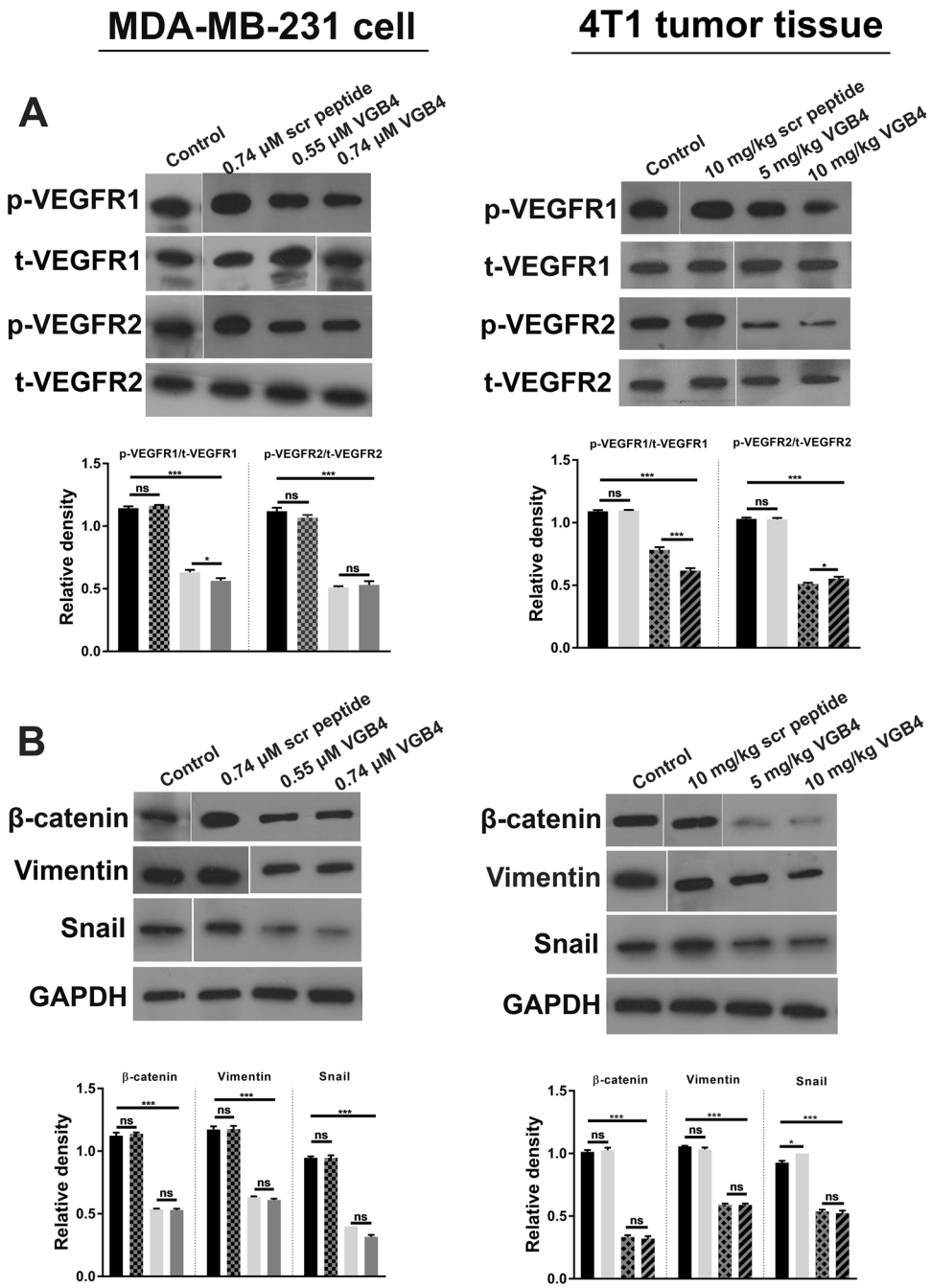

Fig. 3 The disruption of VEGF intracellular signaling pathway by VGB4. **a** MDA-MB-231 cells or 4T1 tumor tissues were treated with different concentrations of VGB4 or scr and then lysates were subjected to western blot to analyze the expression levels of phosphorylated and total forms of VEGFR1 and VEGFR2. **b** MDA-MB-231 cells or 4T1 tumor tissues treated with different concentrations of VGB4 or scr were subjected to western blot to analyze the expression levels of β-catenin, Vimentin and Snail. GAPDH was used as internal control to quantify the protein bands using image J gel analysis program. Full-length blots are presented in Supplementary Figs. S2 and S3. Data were represented as mean ± SD, n = 3, $^{*}P < 0.05$, $^{***}P < 0.001$ versus the control groups

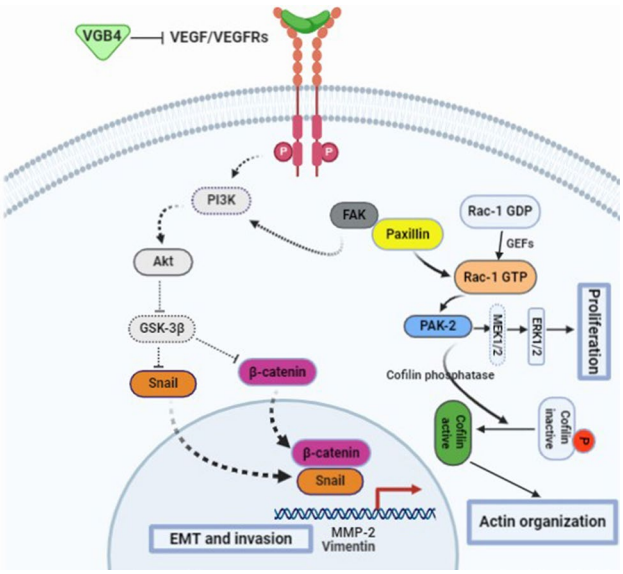

Fig. 4 Schematic representation of VEGF downstream signaling pathways related to migration and invasion. In this model, VGB4, interfering VEGF/VEGFRs interaction, inhibits proliferation, actin organization, and EMT process through inactivating RAC1-PAK2-Cofilin pathway and FAK-Paxillin-MMP2 pathway

VEGF/VEGFR2 axis promotes cells proliferation, often via canonical MAPK/ERK signaling, and cells migration, vascular permeability, and cells survival through FAK/PI3K/Akt signaling pathway [36], and VEGF/VEGFR1 axis induces proliferation, migration, and invasion of tumor cells through MAPK/ERK and PI3K/Akt/Rac1 signaling pathways [37]. EMT-inducing signaling pathways through VEGFR1 and VEGFR2 drives tumor progression, invasion, and metastasis with a gain of mesenchymal markers, such as Vimentin [38, 39]. We previously demonstrated that VGB4 could interfere with VEGF/VEGFRs interaction and their downstream signaling pathways [24]. In the current study, we investigated in more details the effect of VGB4 on signaling pathways of migration and invasion. VGB4 inhibited VEGF-induced HUVECs and MDA-MB-231 cells proliferation dose- and time- dependently. Likewise, VEGF-induced HUVECs and MDA-MB-231 cells migration strongly suppressed by VGB4 for a prolonged time (48 and 72 h). In addition, significant reduction of VEGFR1 and VEGFR2 phosphorylation inactivated FAK-Paxillin-MMP-2 as well as Rac-PAK-Cofilin pathways in VGB4-treated tumor tissues (Fig. 4). Meanwhile, a marked decrease in Vimentin, β-catenin and Snail levels (as EMT markers) was observed in VGB4-treated MDA-MB-231 cells and VGB4-treated 4T1 tumors.

In tumor tissues, organization of the adhesion complexes and actin cytoskeleton promotes cancer cell migration and invasion [40]. Many studies have shown that high levels of FAK correlate with increased malignancy and invasiveness [41, 42], and loss of FAK reduces invasion degree of breast cancer cells [43]. The binding of VEGF to VEGFR2 triggers FAK activation, which is required for the recruitment of paxillin to FAK in focal adhesion site, leading to the cytoskeletal reorganization and cell migration [44, 45]. Rac1 and PAK-2 are also highly expressed in different tumors and contributes to the invasion of breast cancer cells, and activated through VEGFR2 and induces stress fiber formation and cancer cell migration [46, 47]. Likewise, the activity of cofilin pathway is known as an important determinant of tumor cell metastatic and invasive phenotype [48]. In tumor cells, VEGF-stimulated VEGFR2-Y1175 and VEGFR1-Y1333 phosphorylation create a binding site for phospholipase Cγ (PLCγ) [49, 50]. Activated PLCγ hydrolyses phosphatidylinositol 4,5-bisphosphate (PIP2) resulting in release of cofilin (which is in complex with PIP2) from the cell membrane, and cofilin phosphorylation by LIMK led to the cell protrusion and motility [48]. Our western blot analysis showed a strong reduction of phosphorylated VEGFR1 and VEGFR2 in VGB4-treated MDA-MB-231 cells and VGB4-treated 4T1 tumors. A statistically significant reduction in mRNA level of FAK, Paxillin, Rac1, PAK-2 and Cofilin-1 was also observed in VGB4-treated tumor tissue sections. These results indicate that VGB4 down-regulated the canonical pathways of VEGF-VEGFR1/2 signaling associated with cancer migration and metastasis. Furthermore, the noticeable decreased MMP-2, as well as Vimentin, β-catenin and Snail levels observed in current study is in accordance with increased E-cadherin expression, and reduced N-cadherin, NF-KB, and MMP-9 expression observed in our previous study. Taken together, the results of this study suggest potential application of VGB4 to effectively arrest tumor growth and metastasis through the blockade of VEGFR1 and VEGFR2 phosphorylation followed by inactivation of a wide range of signal transduction mediators.

Compliance with ethical standards

Conflict of interest The authors declare that they have no conflict of interest.

References

1. Bielenberg DR, Zetter BR (2015) The contribution of angiogenesis to the process of metastasis. Cancer J 21(4):267. https://doi.org/10.1097/PPO.0000000000000138
2. Lauffenburger DA, Horwitz AF (1996) Cell migration: a physically integrated molecular process. Cell 84(3):359–369. https://doi.org/10.1016/S0092-8674(00)81280-5

3. Ivaska J, Heino J (2010) Interplay between cell adhesion and growth factor receptors: from the plasma membrane to the endosomes. Cell Tissue Res 339(1):111. https://doi.org/10.1007/s00441-009-0857-z
4. Avraham HK, Lee T-H, Koh Y, Kim T-A, Jiang S, Sussman M, Samarel AM, Avraham S (2003) Vascular endothelial growth factor regulates focal adhesion assembly in human brain microvascular endothelial cells through activation of the focal adhesion kinase and related adhesion focal tyrosine kinase. J Biol Chem 278(38):36661–36668. https://doi.org/10.1074/jbc.M301253200
5. Abedi H, Zachary I (1997) Vascular endothelial growth factor stimulates tyrosine phosphorylation and recruitment to new focal adhesions of focal adhesion kinase and paxillin in endothelial cells. J Biol Chem 272(24):15442–15451. https://doi.org/10.1074/jbc.272.24.15442
6. Mitra SK, Hanson DA, Schlaepfer DD (2005) Focal adhesion kinase: in command and control of cell motility. Nat Rev Mol Cell Biol 6(1):56. https://doi.org/10.1038/nrm1549
7. Golubovskaya V, Beviglia L, Xu L-H, Earp HS, Craven R, Cance W (2002) Dual inhibition of focal adhesion kinase and epidermal growth factor receptor pathways cooperatively induces death receptor-mediated apoptosis in human breast cancer cells. J Biol Chem 277(41):38978–38987. https://doi.org/10.1074/jbc.M205002200
8. Sieg DJ, Hauck CR, Ilic D, Klingbeil CK, Schaefer E, Damsky CH, Schlaepfer DD (2000) FAK integrates growth-factor and integrin signals to promote cell migration. Nat Cell Biol 2(5):249. https://doi.org/10.1038/35010517
9. Mon NN, Ito S, Senga T, Hamaguchi M (2006) FAK signaling in neoplastic disorders: a linkage between inflammation and cancer. Ann N Y Acad Sci 1086(1):199–212. https://doi.org/10.1196/annals.1377.019
10. Hu Y-L, Lu S, Szeto KW, Sun J, Wang Y, Lasheras JC, Chien S (2014) FAK and paxillin dynamics at focal adhesions in the protrusions of migrating cells. Sci Rep 4:6024. https://doi.org/10.1038/srep06024
11. Brown MC, Turner CE (2004) Paxillin: adapting to change. Physiol Rev 84(4):1315–1339. https://doi.org/10.1152/physrev.00002.2004
12. Kumar R, Gururaj AE, Barnes CJ (2006) p21-activated kinases in cancer. Nat Rev Cancer 6(6):459. https://doi.org/10.1038/nrc1892
13. Renkema GH, Pulkkinen K, Saksela K (2002) Cdc42/Rac1-mediated activation primes PAK2 for superactivation by tyrosine phosphorylation. Mol Cell Biol 22(19):6719–6725. https://doi.org/10.1128/MCB.22.19.6719-6725.2002
14. Mira J-P, Benard V, Groffen J, Sanders LC, Knaus UG (2000) Endogenous, hyperactive Rac3 controls proliferation of breast cancer cells by a p21-activated kinase-dependent pathway. Proc Natl Acad Sci 97(1):185–189. https://doi.org/10.1073/pnas.97.1.185
15. Holm C, Rayala S, Jirström K, Stål O, Kumar R, Landberg G (2006) Association between Pak1 expression and subcellular localization and tamoxifen resistance in breast cancer patients. J Natl Cancer Inst 98(10):671–680. https://doi.org/10.1093/jnci/djj185
16. Arias-Romero LE, Chernoff J (2010) p21-activated kinases in Erbb2-positive breast cancer: A new therapeutic target? Small GTPases 1(2):5839–5849. https://doi.org/10.4161/sgtp.1.2.14109
17. Maekawa M, Ishizaki T, Boku S, Watanabe N, Fujita A, Iwamatsu A, Obinata T, Ohashi K, Mizuno K, Narumiya S (1999) Signaling from Rho to the actin cytoskeleton through protein kinases ROCK and LIM-kinase. Science 285(5429):895–898. https://doi.org/10.1126/science.285.5429.895
18. Delorme V, Machacek M, DerMardirossian C, Anderson KL, Wittmann T, Hanein D, Waterman-Storer C, Danuser G, Bokoch GM (2007) Cofilin activity downstream of Pak1 regulates cell protrusion efficiency by organizing lamellipodium and lamella actin networks. Dev Cell 13(5):646–662. https://doi.org/10.1016/j.devcel.2007.08.011
19. Rider L, Oladimeji P, Diakonova M (2013) PAK1 regulates breast cancer cell invasion through secretion of matrix metalloproteinases in response to prolactin and three-dimensional collagen IV. Mol Endocrinol 27(7):1048–1064. https://doi.org/10.1210/me.2012-1322
20. Poola I, DeWitty RL, Marshalleck JJ, Bhatnagar R, Abraham J, Leffall LD (2005) Identification of MMP-1 as a putative breast cancer predictive marker by global gene expression analysis. Nat Med 11(5):481. https://doi.org/10.1038/nm1243
21. Lu P, Takai K, Weaver VM, Werb Z (2011) Extracellular matrix degradation and remodeling in development and disease. Cold Spring Harb Perspect Biol 3(12):a005058. https://doi.org/10.1101/cshperspect.a005058
22. Smith BN, Burton LJ, Henderson V, Randle DD, Morton DJ, Smith BA, Taliaferro-Smith L, Nagappan P, Yates C, Zayzafoon M (2014) Snail promotes epithelial mesenchymal transition in breast cancer cells in part via activation of nuclear ERK2. PLoS ONE 9(8):e104987. https://doi.org/10.1371/journal.pone.0104987
23. Liu C-Y, Lin H-H, Tang M-J, Wang Y-K (2015) Vimentin contributes to epithelial-mesenchymal transition cancer cell mechanics by mediating cytoskeletal organization and focal adhesion maturation. Oncotarget 6(18):15966
24. Behelgardi MF, Zahri S, Mashayekhi F, Mansouri K, Asghari SM (2018) A peptide mimicking the binding sites of VEGF-A and VEGF-B inhibits VEGFR-1/-2 driven angiogenesis, tumor growth and metastasis. Sci Rep 8(1):17924. https://doi.org/10.1038/s41598-018-36394-0
25. Bauer AT, Bürgers HF, Rabie T, Marti HH (2010) Matrix metalloproteinase-9 mediates hypoxia-induced vascular leakage in the brain via tight junction rearrangement. J Cerebral Blood Flow Metab 30(4):837–848. https://doi.org/10.1038/jcbfm.2009.248
26. Lee JH, Shim JW, Choi YJ, Heo K, Yang K (2013) The combination of sorafenib and radiation preferentially inhibits breast cancer stem cells by suppressing HIF-1α expression. Oncol Rep 29(3):917–924. https://doi.org/10.3892/or.2013.2228
27. Goel HL, Mercurio AM (2013) VEGF targets the tumour cell. Nat Rev Cancer 13(12):871. https://doi.org/10.1038/nrc3627
28. Yan J-D, Liu Y, Zhang Z-Y, Liu G-Y, Xu J-H, Liu L-Y, Hu Y-M (2015) Expression and prognostic significance of VEGFR-2 in breast cancer. Pathol Res Pract 211(7):539–543. https://doi.org/10.1016/j.prp.2015.04.003
29. Wang Y, Shi J, Chai K, Ying X, Zhou P (2013) The role of Snail in EMT and tumorigenesis. Curr Cancer Drug Targets 13(9):963–972
30. Luo M, Hou L, Li J, Shao S, Huang S, Meng D, Liu L, Feng L, Xia P, Qin T (2016) VEGF/NRP-1axis promotes progression of breast cancer via enhancement of epithelial-mesenchymal transition and activation of NF-κB and β-catenin. Cancer Lett 373(1):1–11. https://doi.org/10.1016/j.canlet.2016.01.010
31. Ning Q, Liu C, Hou L, Meng M, Zhang X, Luo M, Shao S, Zuo X, Zhao X (2013) Vascular endothelial growth factor receptor-1 activation promotes migration and invasion of breast cancer cells through epithelial-mesenchymal transition. PLoS ONE 8(6):e65217. https://doi.org/10.1371/journal.pone.0065217
32. Gille J, Heidenreich R, Pinter A, Schmitz J, Boehme B, Hicklin DJ, Henschler R, Breier G (2007) Simultaneous blockade of VEGFR-1 and VEGFR-2 activation is necessary to efficiently inhibit experimental melanoma growth and metastasis formation. Int J Cancer 120(9):1899–1908. https://doi.org/10.1002/ijc.22531

33. Sadremomtaz A, Mansouri K, Alemzadeh G, Safa M, Rastaghi AE, Asghari SM (2018) Dual blockade of VEGFR1 and VEGFR2 by a novel peptide abrogates VEGF-driven angiogenesis, tumor growth, and metastasis through PI3K/AKT and MAPK/ERK1/2 pathway. Biochimica et Biophysica Acta (BBA) 1862(12):2688–2700. https://doi.org/10.1016/j.bbagen.2018.08.013
34. Sadremomtaz A, Kobarfard F, Mansouri K, Mirzanejad L, Asghari SM (2018) Suppression of migratory and metastatic pathways via blocking VEGFR1 and VEGFR2. J Recept Signal Trans 38(5–6):432–441. https://doi.org/10.1080/10799893.2019.1567785
35. Assareh E, Mehrnejad F, Mansouri K, Rastaghi ARE, Naderi-Manesh H, Asghari SM (2019) A cyclic peptide reproducing the α1 helix of VEGF-B binds to VEGFR-1 and VEGFR-2 and inhibits angiogenesis and tumor growth. Biochem J 476(4):645–663. https://doi.org/10.1042/BCJ20180823
36. Shiojima I, Walsh K (2002) Role of Akt signaling in vascular homeostasis and angiogenesis. Circ Res 90(12):1243–1250. https://doi.org/10.1161/01.RES.0000022200.71892.9F
37. Wang F, Yamauchi M, Muramatsu M, Osawa T, Tsuchida R, Shibuya M (2011) RACK1 regulates VEGF/Flt1-mediated cell migration via activation of a PI3K/Akt pathway. J Biol Chem 286(11):9097–9106. https://doi.org/10.1074/jbc.M110.165605
38. Butti R, Das S, Gunasekaran VP, Yadav AS, Kumar D, Kundu GC (2018) Receptor tyrosine kinases (RTKs) in breast cancer: signaling, therapeutic implications and challenges. Mol Cancer 17(1):34. https://doi.org/10.1186/s12943-018-0797-x
39. Wei Z, Shan Z, Shaikh ZA (2018) Epithelial-mesenchymal transition in breast epithelial cells treated with cadmium and the role of Snail. Toxicol Appl Pharmacol 344:46–55. https://doi.org/10.1016/j.taap.2018.02.022
40. Nagano M, Hoshino D, Koshikawa N, Akizawa T, Seiki M (2012) Turnover of focal adhesions and cancer cell migration. Int J Cell Biol. https://doi.org/10.1155/2012/310616
41. Sood AK, Coffin JE, Schneider GB, Fletcher MS, DeYoung BR, Gruman LM, Gershenson DM, Schaller MD, Hendrix MJ (2004) Biological significance of focal adhesion kinase in ovarian cancer: role in migration and invasion. Am J Pathol 165(4):1087–1095. https://doi.org/10.1016/S0002-9440(10)63370-6
42. Megison ML, Stewart JE, Nabers HC, Gillory LA, Beierle EA (2013) FAK inhibition decreases cell invasion, migration and metastasis in MYCN amplified neuroblastoma. Clin Exp Metas 30(5):555–568. https://doi.org/10.1007/s10585-012-9560-7
43. Wendt MK, Schiemann WP (2009) Therapeutic targeting of the focal adhesion complex prevents oncogenic TGF-β signaling and metastasis. Breast Cancer Res 11(5):R68. https://doi.org/10.1186/bcr2360
44. Rousseau S, Houle F, Kotanides H, Witte L, Waltenberger J, Landry J, Huot J (2000) Vascular endothelial growth factor (VEGF)-driven actin-based motility is mediated by VEGFR2 and requires concerted activation of stress-activated protein kinase 2 (SAPK2/p38) and geldanamycin-sensitive phosphorylation of focal adhesion kinase. J Biol Chem 275(14):10661–10672. https://doi.org/10.1074/jbc.275.14.10661
45. Le Boeuf F, Houle F, Huot J (2004) Regulation of vascular endothelial growth factor receptor 2-mediated phosphorylation of focal adhesion kinase by heat shock protein 90 and Src kinase activities. J Biol Chem 279(37):39175–39185. https://doi.org/10.1074/jbc.M405493200
46. Lamalice L, Houle F, Huot J (2006) Phosphorylation of Tyr1214 within VEGFR-2 triggers the recruitment of Nck and activation of Fyn leading to SAPK2/p38 activation and endothelial cell migration in response to VEGF. J Biol Chem 281(45):34009–34020. https://doi.org/10.1074/jbc.M603928200
47. Zhu X, Zhou W (2015) The emerging regulation of VEGFR-2 in triple-negative breast cancer. Front Endocrinol 6:159. https://doi.org/10.3389/fendo.2015.00159
48. Wang W, Eddy R, Condeelis J (2007) The cofilin pathway in breast cancer invasion and metastasis. Nat Rev Cancer 7(6):429. https://doi.org/10.1038/nrc2148
49. Sawano A, Takahashi T, Yamaguchi S, Shibuya M (1997) The phosphorylated 1169-tyrosine containing region of flt-1 kinase (VEGFR-1) is a major binding site for PLCγ. Biochem Biophys Res Commun 238(2):487–491. https://doi.org/10.1006/bbrc.1997.7327
50. Takahashi T, Yamaguchi S, Chida K, Shibuya M (2001) A single autophosphorylation site on KDR/Flk-1 is essential for VEGF-A-dependent activation of PLC-γ and DNA synthesis in vascular endothelial cells. EMBO J 20(11):2768–2778. https://doi.org/10.1093/emboj/20.11.2768